Hydroxylated Uio-66 Based Quartz Crystal Microbalance Gas Sensor for Carbon Dioxide Detection

Junyi Lin [1, 2, *], He Wang [1, 2], Bofeng Luo [2], Liang Zhao [2], Jiguang Zhao [2],

Qiancheng Lv [2], Zhengkai Li [2], Zhenliang Ye [2], Hao Yang [1, 2]

[1] CSG Digital Power Grid Research Institute Co., Ltd., Guangzhou Guangdong, 510700, China

[2] CSG Sensing Technology (Guangdong) Co., Ltd., Shenzhen Guangdong, 518102, China

* Corresponding Author: Junyi Lin

Abstract. The detection of carbon dioxide (CO_2) is crucial for monitoring climate change, ensuring air quality, managing industrial processes, and safeguarding human health. However, the chemical inertness and stability of CO_2 pose significant challenges to the advancement of detection technologies. To address this, a pre-synthetic modification strategy was employed to introduce hydroxyl (–OH) groups into UiO-66, resulting in the successful preparation of hydroxyl-functionalized UiO-66 for effective CO_2 detection. Sensing results demonstrated that, compared with pristine UiO-66, the quartz crystal microbalance (QCM) CO_2 sensor based on hydroxyl-functionalized UiO-66 exhibited enhanced gas sensing performance, including a sensitivity of 40.3 Hz to 1000 ppm CO_2, response/recovery times of 55 s/58 s, and good selectivity at room temperature.

Keywords: Metal Organic Framework; Quartz Crystal Microbalance; Carbon Dioxide Gas Sensor.

1. Introduction

Carbon dioxide (CO_2) is one of the major greenhouses gases.CO_2 also plays a vital role in human metabolism and plant growth [1,2]. When its concentration exceeds certain thresholds, it can severely affect ecosystems, human health, and agricultural productivity. With the continuous increase in global CO_2 emissions, atmospheric CO_2 concentrations are rising year by year, intensifying the greenhouse effect and leading to global climate change and frequent extreme weather events. CO_2 is also a primary byproduct of human metabolism. When indoor CO_2 levels exceed 5000 ppm, symptoms such as headache and impaired consciousness may occur, and in severe cases, respiratory acidosis or even life-threatening conditions can develop [3]. Furthermore, CO_2 is a raw material for photosynthesis in plants, and deviations from the optimal concentration can affect both respiration and photosynthesis, ultimately compromising plant quality and agricultural output, as well as disturbing ecological balance [4,5].

Gas detection and monitoring technologies are of great importance in environmental protection, human health, and agricultural production. There is an urgent need to develop efficient, sensitive, and miniaturized CO_2 gas sensors for real-time monitoring of CO_2 concentration variations. However, due to the chemical inertness of CO_2 and its resistance to redox reactions under ambient conditions, conventional metal oxide sensors are ineffective for its detection. Optical sensors offer high precision but are relatively costly. Gas chromatography provides excellent selectivity but suffers from long analysis time and bulky instrumentation. Electrochemical sensors are low-cost but lack selectivity. Quartz crystal microbalance (QCM) gas sensors, as mass-sensitive devices, offer outstanding sensitivity, rapid response, and miniaturization potential, making them highly promising for gas detection applications. Compared with other types of gas sensors, QCM sensors can achieve high-precision detection by monitoring the mass change induced by gas molecule adsorption on the sensor surface, showing excellent potential for detecting inert gases [6]. The integration of materials with excellent adsorption properties into QCM devices is beneficial for tuning the sensing performance. Metal-organic frameworks (MOFs), as a new class of porous materials, are characterized by high surface area, large porosity, and diverse topologies. The performance of QCM-based CO_2 sensors can be enhanced through rational design of MOF or COF structures, ligands, or composite components.

In this work, hydroxyl-functionalized UiO-66 and pristine UiO-66 were successfully synthesized via a one-pot method. The gas sensing performance of QCM-based CO_2 sensors fabricated with both materials was comparatively studied. The results demonstrate that the hydroxylated UiO-66 sensor exhibits superior sensing properties toward CO_2. Finally, the mechanism underlying the enhanced gas sensing performance due to hydroxylation was analyzed.

2. Experiment

2.1 Reagents and Instruments

Analytical grade zirconium chloride ($ZrCl_4$), terephthalic acid (H_2BDC), and 2-hydroxyterephthalic acid (BDC-OH) were purchased from Aladdin Reagent Co., Ltd. (Shanghai, China). N,N-dimethylformamide (DMF) and acetic acid, also of analytical grade, were obtained from Sinopharm Chemical Reagent Co., Ltd. The crystalline structures of the synthesized materials were characterized using an X-ray diffractometer (XRD, Rigaku D/Max-2550). Fourier transform infrared (FT-IR) spectra were recorded with a Thermo Nicolet 550 spectrometer. The specific surface area and pore size distribution were determined by nitrogen adsorption measurements using a JW-BK132F surface area analyzer.

2.2 Synthesis of Hydroxylated UiO-66

0.1 mmol of $ZrCl_4$ was dissolved in 5 mL of DMF, and 0.1 mmol of BDC-OH was dissolved in another 5 mL of DMF. The two solutions were combined in a 20 mL glass vial, followed by the addition of 0.5 mL acetic acid. The sealed vial was heated at 120 °C for 24 hours. The resulting product was collected by centrifugation, washed sequentially with DMF and methanol, and then dried under vacuum at 60 °C to obtain hydroxylated UiO-66 (UiO-66-OH) powder.

2.3 Synthesis of UiO-66

0.1 mmol of $ZrCl_4$ was dissolved in 5 mL of DMF, and 0.1 mmol of H_2BDC was dissolved in another 5 mL of DMF. The two solutions were mixed in a 20 mL glass vial, to which 0.5 mL of acetic acid was added. After sealing, the vial was heated at 120 °C for 24 hours. The obtained product was collected via centrifugation, washed with DMF and methanol, and vacuum-dried at 60 °C to yield UiO-66 powder.

2.4 Fabrication of QCM Sensor

The fabrication of the QCM sensor involved three main steps: cleaning of the QCM substrate, coating of the sensing film, and aging. The QCM surface was first cleaned using either piranha solution or a mixture of acetone and ethanol under ultrasonic conditions to remove surface impurities and organic contaminants, followed by drying under a nitrogen stream [7]. The sensing material was then dispersed in ethanol at a concentration of 1 mg/mL to prepare a uniform suspension. A micropipette was used to drop the suspension onto the center of the QCM electrode surface. Finally, the coated sensor was dried in a vacuum oven or under an infrared lamp to form a uniform sensitive film, improving the adhesion between the sensing material and the QCM substrate, thereby enhancing the stability of the sensor. The QCM sensor functionalized with the sensing material was thus successfully fabricated.

2.5 Construction of the Testing System

CO_2 gas was introduced into the test chamber using a dynamic gas mixing system. Eight independent mass flow controllers were used to regulate the flow rates of the background gas (N_2) and the standard gas (CO_2). After homogenization in a mixing chamber, the resulting gas mixture with varying CO_2 concentrations was delivered to the test chamber at a constant flow rate of 500 mL/min. The test chamber consisted of a QCM sensor holder and a sealed chamber with a total

volume of 30 mL. The holder fixed the QCM sensor in place to minimize mechanical vibrations and signal drift. When the target gas entered the chamber, the QCM sensor responded to CO_2 adsorption by exhibiting a mass increase, which resulted in a decrease in resonant frequency. After the sensor frequency stabilized in the presence of CO_2, the target gas was replaced with background gas (N_2) to induce desorption. A CO_2 detector (Dynament) was installed at the outlet of the test chamber to continuously monitor and calibrate the CO_2 concentration in real-time. After each testing cycle, the QCM sensor was placed in a vacuum oven at 80 °C for 1 hour to thermally regenerate the sensing material, enabling repeated use.

All gas sensing tests of the QCM sensors were conducted at room temperature. Frequency signals were acquired using an oscillator circuit. The QCM sensors were driven by an excitation circuit, and the resonance frequency shift was monitored in real time by a frequency counter (53220A, Keysight) and recorded through a computer interface.

3. Results and Discussion

3.1 Structural Characterization of the Materials

The crystallinity and phase purity of UiO-66 and hydroxylated UiO-66 were investigated by X-ray diffraction (XRD), as shown in Figure 1. Both materials exhibit characteristic diffraction peaks that match well with the standard pattern of UiO-66, indicating successful synthesis with high crystallinity and phase purity. Moreover, the hydroxylated UiO-66 maintains the same structural framework as pristine UiO-66, suggesting that the hydroxylation process does not disrupt the original crystalline structure.

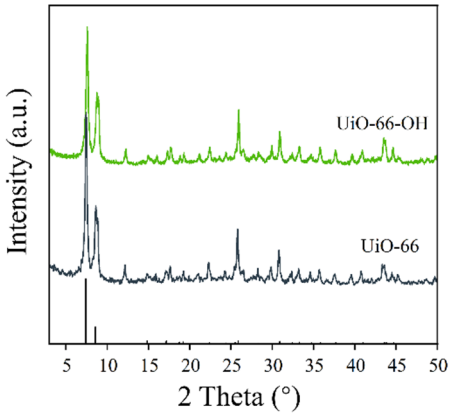

Fig 1. XRD patterns of UiO-66 and hydroxylated UiO-66

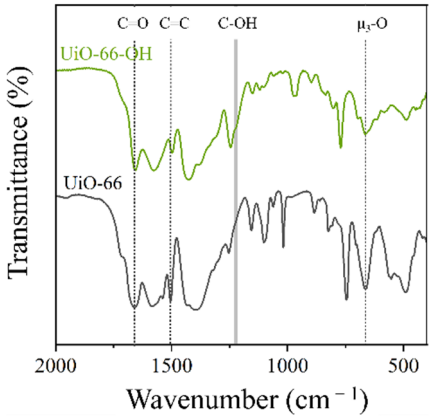

Fig 2. FT-IR spectra of UiO-66 and hydroxylated UiO-66

Figure 2 presents the FT-IR spectra of UiO-66 and hydroxylated UiO-66. The stretching vibration peak of μ_3-O in Zr-(OC) bonds appears at 660 cm^{-1}, confirming the coordination between the metal centers and organic ligands. The peak at 1502 cm^{-1} corresponds to the C=C stretching vibration in the benzene ring of the ligand, indicating the existence of the organic framework. The C=O stretching vibration peak at 1660 cm^{-1} further confirms the presence of carboxylic acid groups. Notably, the absorption peak near 1230 cm^{-1} suggests the presence of phenolic hydroxyl groups (–OH), which can serve as active adsorption sites for CO_2 molecules, thereby enhancing the CO_2 capture capability of the material [8,9].

To evaluate the porosity of the materials, N_2 adsorption–desorption isotherms were recorded (Figure 3A). Both UiO-66 and hydroxylated UiO-66 exhibit typical type I isotherms, indicating their microporous nature. BET surface area analysis reveals values of 648 m^2/g and 604 m^2/g for UiO-66 and hydroxylated UiO-66, respectively. The corresponding pore size distributions show average pore diameters of 8.0 Å for UiO-66 and 7.2 Å for hydroxylated UiO-66 (Figure 3B and 3C).

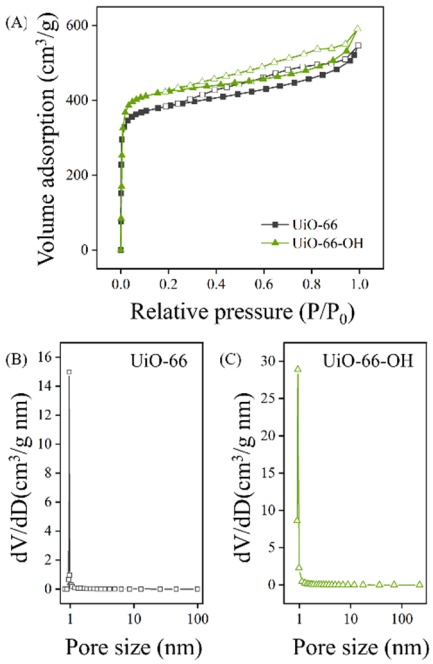

Fig 3. (A) N_2 adsorption–desorption isotherms, (B) pore size distribution of UiO-66, (C) pore size distribution of hydroxylated UiO-66

3.2 CO_2 Gas Sensing Performance

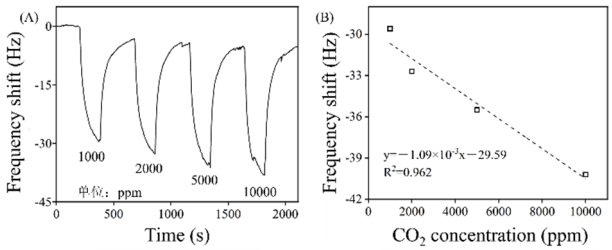

Fig 4. (A) Dynamic response and recovery curves to CO_2 and (B) response vs. CO_2 concentration of hydroxylated UiO-66

Hydroxyl groups (–OH) are polar and nucleophilic, which significantly enhances the adsorption capacity of the material towards CO_2 and, consequently, improves the sensitivity of the QCM sensor. In this study, QCM sensors based on UiO-66 and hydroxylated UiO-66 were fabricated and tested

for CO_2 sensing. The frequency shift (Δf), defined as the difference between the sensor frequency in the target gas (f_g) and in the baseline gas (f_0), was used to evaluate sensor performance:

$$\Delta f = f_g - f_0$$

The gas sensing behavior of the hydroxylated UiO-66 sensor was studied under CO_2 concentrations ranging from 1000 to 10000 ppm at room temperature and 40% RH. As shown in Figure 4A, the frequency decreases notably upon exposure to CO_2, with the magnitude of the response increasing alongside CO_2 concentration. The frequency responses at 1000, 2000, 5000, and 10000 ppm CO_2 were −30.6, −32.7, −35.5, and −40.2 Hz, respectively. Figure 4B illustrates a good linear relationship between CO_2 concentration and sensor response, indicating efficient adsorption and interaction with CO_2 molecules.

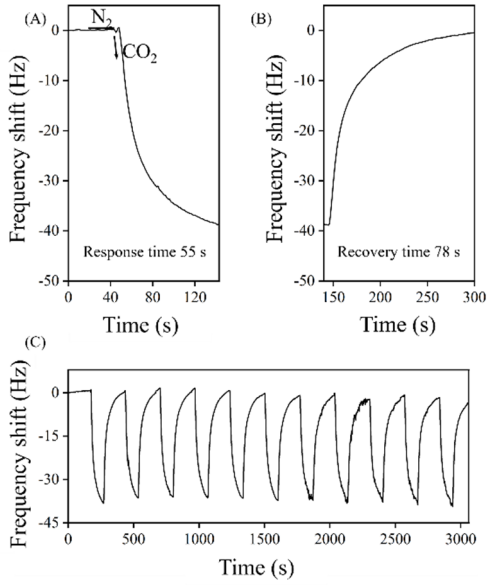

Fig 5. (A) Response time, (B) recovery time, (C) repeatability at 10000 ppm CO_2 of the hydroxylated UiO-66 sensor

The response time (time to reach 90% of the maximum response upon gas exposure) and recovery time (time to return to 90% of the baseline upon removal of CO_2) were determined to be 55 s and 58 s, respectively, as shown in Figure 5A and 5B. Repeatability tests demonstrated consistent response behavior over multiple cycles, indicating excellent stability and reproducibility (Figure 5C).

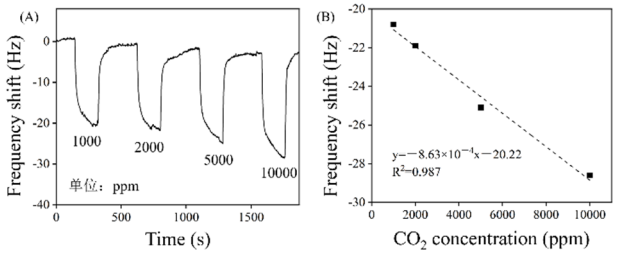

Fig 6. (A) Dynamic response and recovery curves to CO_2 and (B) response vs. CO_2 concentration of UiO-66

For comparison, the sensing performance of the pristine UiO-66 sensor was also evaluated under identical conditions. Figure 6A shows the dynamic response curves. The frequency shifts at 1000, 2000, 5000, and 10000 ppm CO_2 were −20.8, −21.9, −25.1, and −28.6 Hz, respectively. As shown in Figure 6B, a good linear correlation was observed between CO_2 concentration and frequency response.

The response and recovery times of the UiO-66 sensor at 10000 ppm CO_2 were 55 s and 49 s, respectively, as shown in Figures 7A and 7B. The repeatability test confirmed good stability over eight cycles (Figure 7C).

In this study, sensitivity (S) is defined as the absolute value of the frequency shift:

$$S = \left| f_g - f_0 \right|$$

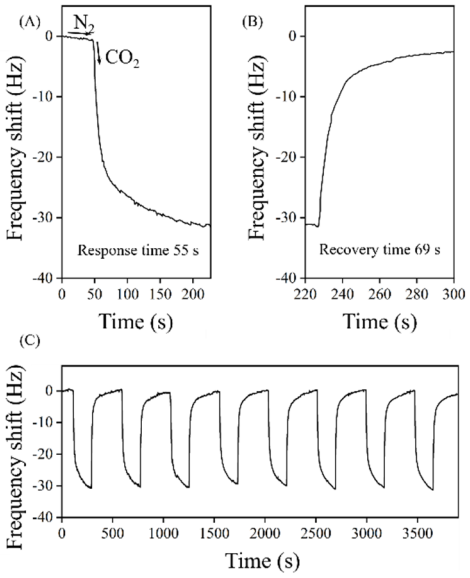

Fig 7. (A) Response time, (B) recovery time, (C) repeatability at 10000 ppm CO_2 of the UiO-66 sensor

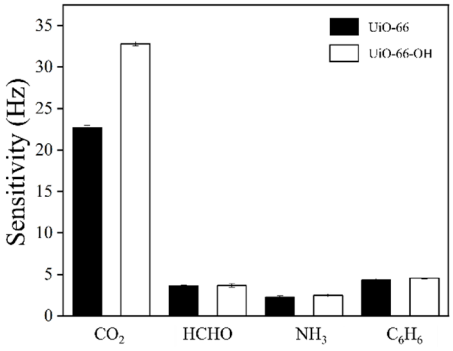

Fig 8. Selectivity of UiO-66 and hydroxylated UiO-66 sensors

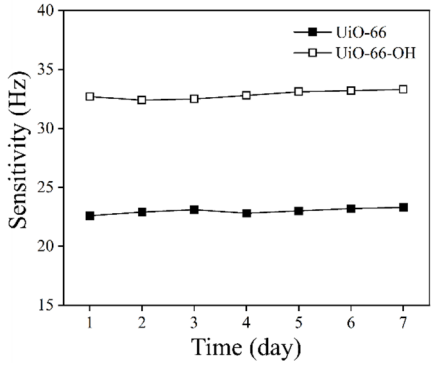

Fig 9. Long-term stability of the sensors in 2000 ppm CO_2

Figure 8 compares the selectivity of the two sensors towards various indoor air pollutants. The CO_2 concentration was set at 2000 ppm, while HCHO, NH_3, and C_6H_6 were each at 100 ppm. Both sensors exhibited superior sensitivity to CO_2, demonstrating good selectivity and potential for distinguishing CO_2 from other interfering gases.

The long-term stability of the sensors was evaluated over a 7-day period under 2000 ppm CO_2. As shown in Figure 9, both sensors maintained stable responses with minimal drift or performance degradation, confirming their reliability for extended operation.

3.3 Sensing Mechanism

Hydroxyl groups (–OH) are known to serve as active sites for CO_2 adsorption due to their polarity and nucleophilicity [10–13]. For instance, Winston et al. enhanced CO_2 adsorption of CFA-1 by incorporating –OH groups via ligand exchange [14]. Ibarra et al. reported that –OH groups on CAU-10 improved its CO_2 capture capacity by 1.3 times [15]. Similarly, Z. Li et al. confirmed via CO_2-TPD and in situ FT-IR that –OH groups in MIL-100(Fe) facilitated CO_2 adsorption and selectivity [16].

In this work, –OH groups were introduced into UiO-66 through pre-synthetic modification, enhancing its CO_2 adsorption capacity and thereby increasing the mass loading of the QCM sensing layer, which contributes to improved sensitivity. Both UiO-66 and hydroxylated UiO-66 possess high specific surface areas, facilitating effective adsorption–desorption interactions with CO_2 molecules. Density Functional Theory (DFT) calculations have revealed that the interaction strength between CO_2 and adsorption sites follows the order: –OH > –O > pore surface [17]. The strong affinity between CO_2 and –OH sites is likely attributed to Coulombic interactions between the negatively charged oxygen atoms in CO_2 and the positively charged hydrogen atoms in hydroxyl groups. Overall, the presence of –OH groups significantly enhances CO_2 adsorption and mass change on the sensor surface, resulting in larger frequency shifts and higher sensitivity [18,19].

4. Conclusion

In summary, the QCM sensor detects target gas molecules by monitoring the resonance frequency shift of the quartz crystal, which is caused by mass changes in the sensing layer upon gas adsorption. This sensing mechanism endows QCM sensors with notable advantages such as rapid response, low detection limits, and operational simplicity. In this study, a pre-synthetic modification strategy was employed to directly introduce hydroxyl (–OH) groups into the framework of UiO-66, resulting in the successful synthesis of hydroxylated UiO-66. The structural changes of the materials were thoroughly characterized using multiple techniques, and a comparative investigation of the CO_2 sensing performance of QCM sensors based on pristine and hydroxylated UiO-66 was conducted at room temperature. The hydroxylated UiO-66-based sensor exhibited a significant response to CO_2 within the tested concentration range of 1000–10000 ppm. Notably, at 1000 ppm CO_2, the sensor demonstrated a sensitivity of 30.6 Hz, which is approximately 1.5 times higher than that of the UiO-66-based sensor. This enhancement in sensitivity is attributed to the strengthened Coulombic interactions between the introduced –OH groups and CO_2 molecules. Hydroxylation proves to be an effective modification strategy for improving CO_2 adsorption capacity, offering a promising approach for the development of efficient room-temperature CO_2 sensors.

References

[1] E. F. Paiva, J. H. Paxton, and B. J. O'Neil, "The use of end-tidal carbon dioxide ($ETCO_2$) measurement to guide management of cardiac arrest: A systematic review," *Resuscitation,* vol. 123, pp. 1-7, Feb 2018, doi: 10.1016/j.resuscitation.2017.12.003.

[2] J. Jouwena, D. Verbeke, A. M. De Wolf, A. Neyrinck, and J. F. A. Hendrickx, "*In Vitro* Model of Prepacked Carbon Dioxide Absorber Use: Development and Testing," *Anesthesiology,* vol. 140, no. 3, pp. 450-462, Mar, 2024.

[3] K. Azuma, N. Kagi, U. Yanagi, and H. Osawa, "Effects of low-level inhalation exposure to carbon dioxide in indoor environments: A short review on human health and psychomotor performance," *Environment International,* vol. 121, pp. 51-56, Dec, 2018.

[4] L. M. Jablonski, X. Z. Wang, and P. S. Curtis, "Plant reproduction under elevated CO_2 conditions: a meta-analysis of reports on 79 crop and wild species," *New Phytologist,* vol. 156, no. 1, pp. 9-26, Oct, 2002.

[5] S. Devi, and N. Gupta, "Dynamics of carbon dioxide gas (CO_2): Effects of varying capability of plants to absorb CO_2," *Natural Resource Modeling,* vol. 32, no. 1, pp. 18, Feb, 2019.

[6] X. K. Wang, X. Y. Xu, T. T. Zhou, and T. Zhang, "Nanoscale MOF-74-based QCM gas sensor for CO2 detection at room temperature," *Sensors and Actuators B-Chemical,* vol. 413, pp. 11, Aug, 2024.

[7] A. Alassi, M. Benammar, and D. Brett, "Quartz Crystal Microbalance Electronic Interfacing Systems: A Review," *Sensors,* vol. 17, no. 12, pp. 41, Dec, 2017.

[8] S. S. Chen, J. Liu, Y. F. Xu, Z. Li, T. Wang, J. Xu, and Z. Wang, "Hydrogen storage properties of the novel crosslinked UiO-66-$(OH)_2$," *International Journal of Hydrogen Energy,* vol. 43, no. 32, pp. 15370-15377, Aug, 2018.

[9] F. Sánchez, M. Gutiérrez, and A. Douhal, "Taking Advantage of a Luminescent ESIPT-Based Zr-MOF for Fluorochromic Detection of Multiple External Stimuli: Acid and Base Vapors, Mechanical Compression, and Temperature," *Acs Applied Materials & Interfaces,* vol. 15, no. 48, pp. 56587-56599, Nov, 2023.

[10] J. J. Gassensmith, H. Furukawa, R. A. Smaldone, R. S. Forgan, Y. Y. Botros, O. M. Yaghi, and J. F. Stoddart, "Strong and Reversible Binding of Carbon Dioxide in a Green Metal-Organic Framework," *Journal of the American Chemical Society,* vol. 133, no. 39, pp. 15312-15315, Oct, 2011.

[11] G. Y. Zhang, G. F. Wei, Z. P. Liu, S. R. J. Oliver, and H. H. Fei, "A Robust Sulfonate-Based Metal-Organic Framework with Permanent Porosity for Efficient CO_2 Capture and Conversion," *Chemistry of Materials,* vol. 28, no. 17, pp. 6276-6281, Sep, 2016.

[12] N. Mosca, R. Vismara, J. A. Fernandes, G. Tuci, C. Di Nicola, K. V. Domasevitch, C. Giacobbe, G. Giambastiani, C. Pettinari, M. Aragones-Anglada, P. Z. Moghadam, D. Fairen-Jimenez, A. Rossin, and S. Galli, "Nitro-functionalized Bis(pyrazolate) Metal-Organic Frameworks as Carbon Dioxide Capture Materials under Ambient Conditions," *Chemistry-a European Journal,* vol. 24, no. 50, pp. 13170-13180, Sep, 2018.

[13] R. A. Smaldone, R. S. Forgan, H. Furukawa, J. J. Gassensmith, A. M. Z. Slawin, O. M. Yaghi, and J. F. Stoddart, "Metal-Organic Frameworks from Edible Natural Products," *Angewandte Chemie-International Edition,* vol. 49, no. 46, pp. 8630-8634, 2010.

[14] C. E. Bien, K. K. Chen, S. C. Chien, B. R. Reiner, L. C. Lin, C. R. Wade, and W. S. W. Ho, "Bioinspired Metal-Organic Framework for Trace CO_2 Capture," *Journal of the American Chemical Society,* vol. 140, no. 40, pp. 12662-12666, Oct, 2018.

[15] V. B. López-Cervantes, E. Sánchez-González, T. Jurado-Vázquez, A. Tejeda-Cruz, E. González-Zamora, and I. A. Ibarra, "CO_2 adsorption under humid conditions: Self-regulated water content in CAU-10," *Polyhedron,* vol. 155, pp. 163-169, Nov, 2018.

[16] H. Wu, Y. S. Chua, V. Krungleviciute, M. Tyagi, P. Chen, T. Yildirim, and W. Zhou, "Unusual and Highly Tunable Missing-Linker Defects in Zirconium Metal-Organic Framework UiO-66 and Their Important Effects on Gas Adsorption," *Journal of the American Chemical Society,* vol. 135, no. 28, pp. 10525-10532, Jul, 2013.

[17] S. K. Xian, J. J. Peng, Z. J. Zhang, Q. B. Xia, H. H. Wang, and Z. Li, "Highly enhanced and weakened adsorption properties of two MOFs by water vapor for separation of CO_2/CH_4 and $CO_2/N<_2$ binary mixtures," *Chemical Engineering Journal,* vol. 270, pp. 385-392, Jun, 2015.

[18] D. S. Li, W. T. Liu, B. Y. Zhu, M. J. Qu, Q. Zhang, Y. Q. Fu, and J. Xie, "Machine Learning-Assisted Multifunctional Environmental Sensing Based on a Piezoelectric Cantilever," Acs Sensors, pp. 11, 2022 Sep, 2022.

[19] K. S. Pasupuleti, M. Reddeppa, S. S. Chougule, N. H. Bak, D. J. Nam, N. Jung, H. D. Cho, S. G. Kim, and M. D. Kim, "High performance langasite based SAW NO_2 gas sensor using 2D g-C_3N_4@TiO_2 hybrid nanocomposite," *Journal of Hazardous Materials,* vol. 427, pp. 12, Apr, 2022.